


Role of ISM/IGM Energy Balance in Structure Formation and Evolution of Galaxies

F. Tabatabaei^{1,2,3,4} , M. Ghasemi-Nodehi¹, M. Sargent⁵,
E. J. Murphy⁶, E. Schinnerer³, A. Bonaldi⁷ and the SKA ISM/IGM
Focus Group

¹School of Astronomy, Institute for Research in Fundamental Sciences, 19395-5531, Tehran, Iran. email: ftaba@ipm.ir

²Instituto de Astrofísica de Canarias, E-38205 La Laguna, Tenerife, Spain

³Max-Planck-Institut für Astronomie, Königstuhl 17, D-69117 Heidelberg, Germany

⁴Max-Planck Institut für Radioastronomie, Auf dem Hügel 69, 53121 Bonn, Germany

⁵International Space Science Institute (ISSI), Hallerstrasse 6, CH-3012 Bern, Switzerland

⁶National Radio Astronomy Observatory, 520 Edgemont Road, Charlottesville, VA 22903, USA

⁷SKA Organisation, Jodrell Bank, Lower Withington, Macclesfield, Cheshire SK11 9FT, UK

Abstract. Investigating the thermal and non-thermal processes in galaxies is vital to understand their evolution over cosmic time. This can best be studied by combining the radio and optical/near-infrared observations of galaxies. The JWST can resolve the evolution of the thermal processes by mapping ionized gas and dust in distant galaxies. This information combined with the upcoming surveys with the Square Kilometer Array (SKA) will make a major breakthrough in mapping the non-thermal processes and understanding their role in the evolution of galaxies. Our simulations show that SKA surveys will be able to trace the evolution history of spiral galaxies such as M 51 and NGC 6946 back to a redshift of 3 already in its first phase of construction. This study indicates the important role of the non-thermal pressure inserted by cosmic rays and magnetic fields in deriving winds and outflows at cosmic noon as deduced by a flat synchrotron spectrum in star forming galaxies.

Keywords. galaxies: evolution, galaxies: ISM, galaxies: star formation, radio continuum: galaxies

1. Introduction

Observations show that galaxies become redder and less luminous over cosmic time which is linked to the observed deceleration of massive star formation rate (SFR, e.g., [Faber *et al.* 2007](#)). This is explained by a drop in the amount of cold gas fueling star formation through various mechanisms such as feedback and starvation (e.g., [Schaye *et al.* 2015](#), [Peng *et al.* 2015](#)). As such, the cold gas content of galaxies must decrease with time at the same rate as of star formation. However, unresolved ALMA observations of cold gas tracers, such as molecular gas and dust, show that, on average, gas drops at a slower rate than cosmic SFR (e.g., [Tacconi *et al.* 2018](#)). Thus, there has been almost always enough gas to form stars, but for an unknown reason, it has remained quiescent. Resolved studies show that the amount of quiescent gas detected in nearby galaxies depends on the angular resolution ([Schinnerer *et al.* 2019](#)): More gas can be hidden from less resolved

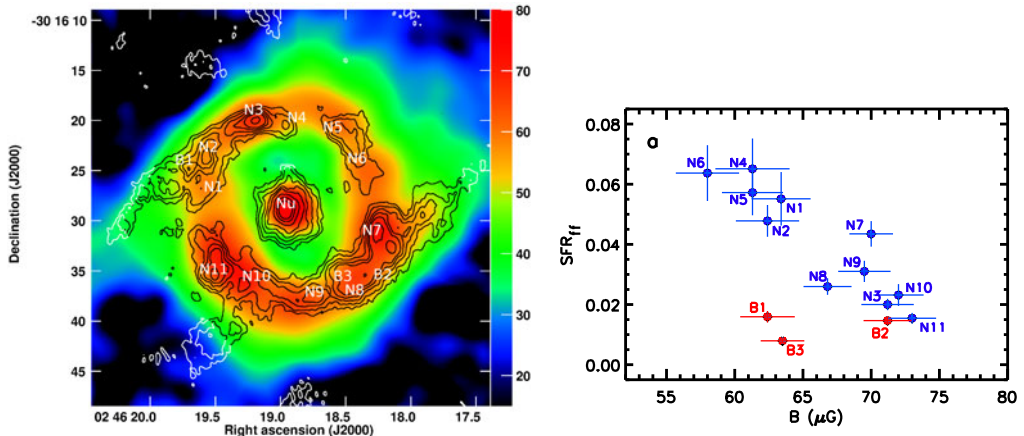


Figure 1. *Left:* Equipartition magnetic field strength (B) in the inner 2 kpc region of NGC1097 in μG units (color scale) with contours of the CO(2-1) line emission overlaid. Contour levels show 3σ , 4σ , 6σ , 8σ , 10σ , 13σ , 17σ , 22σ respectively ($1\sigma=2.3\text{ Jy kms}^{-1}\text{ beam}^{-1}$). Also shown are the narrow-line molecular cloud associations (N1, N2,...) and broad-line ones (B1, B2, B3). *Right:* star formation rate per free-fall SFR_{ff} of the clouds decreases with B in the nuclear ring of NGC 1097 from Tabatabaei *et al.* (2018).

observations. This indicates that the difference between the global dropping rates of the SFR and the cold gas content of galaxies in cosmic time can be even larger than that inferred through unresolved observations. As such, a drop in star formation efficiency of gas clouds must have occurred over cosmic time (e.g., Colombo *et al.* 2020). Important questions are: what does control cold gas against forming stars? and why does the star formation efficiency is reduced over cosmic time? A detailed study of pressure and energy balance in the interstellar medium (ISM) and the intergalactic medium (IGM) is vital to understand factors controlling gas against collapse and accretion over cosmic time.

2. ISM/IGM evolution with JWST & SKA

Observations show that the pressure inserted by cosmic rays and magnetic fields (non-thermal processes) can be higher than the thermal gas pressure in nearby galaxies (e.g., Beck 2007, Hassani *et al.* 2022). The non-thermal processes can control accretion from the IGM (e.g., Owen *et al.* 2013), collapse/fragmentation in the ISM (e.g., Pillai *et al.* 2015), and the star formation rate efficiency of molecular cloud associations (Fig. 1, Tabatabaei *et al.* 2018). The effect of the non-thermal processes on the cosmic evolution of galaxies is a pressing question. These processes can best be traced through the synchrotron continuum radiation observed at the radio frequencies. However, the radio continuum (RC) emission from galaxies is not purely due to synchrotron radiation. Particularly in star-forming regions, the RC emission can be due to the free-free radiation of thermal electrons by about 50% (30%) or even higher at 6 GHz (1 GHz, Tabatabaei *et al.* 2013, 2022). A correction is hence needed to map the synchrotron radiation and to study the thermal and non-thermal processes in galaxies. The traditional method of modeling the radio spectral energy distribution is well suited for global, integrated studies (Condon *et al.* 1991, Tabatabaei *et al.* 2017). In local, resolved studies, this method is mostly insensitive to the diffuse ISM because of its technical challenge. A more ideal and physically motivated technique in resolved galaxy studies combines recombination lines such as de-reddened $\text{H}\alpha$ emission (as free-free templates) with the RC data to map the synchrotron emission, cosmic ray electron energy index, and magnetic field strength (Tabatabaei *et al.* 2013, 2018, Tabatabaei *et al.* 2022). Hence, investigating the

energy balance and the role of the non-thermal processes in the ISM/IGM over cosmic time ideally requires resolved observations in both optical and radio domains. The JWST integral field spectroscopy (IFS) with NIRSpec (Jakobsen *et al.* 2022) provides a 3 square arcsec field of view with a pixel resolution of 0.1 arcsec allowing us to map galaxies in the brightest hydrogen recombination lines back to beyond the peak of the SFR (cosmic noon). At the end of its construction, SKA will be the most powerful radio telescope in the world with an image resolution quality of more than 50 times better than the Hubble Space Telescope while having the ability to image very large areas of the sky. Hence, SKA will perfectly augment and complement the discoveries made by the JWST. In phase 1, SKA will include ~ 197 dishes operating at specific frequency bands between 0.3 and 14 GHz (SKA1-MID) and 131000 antennas operating between 0.05 and 0.3 GHz (SKA1-LOW). In phase 2 of construction, the number of dishes will be increased to thousands and antennas to over a million.

We study the role of the thermal and non-thermal processes in the ISM/IGM energy balance in the SKA era. This is addressed by simulating maps of the RC and HI line emission of nearby star forming galaxy analogs in the past, taking into account the evolution of the SFR (Schreiber *et al.* 2015) and the galaxy size evolution (van der Wel *et al.* 2014). The maps are simulated to resemble those which will be observed with proposed SKA1-MID surveys in band 1 (0.3-1 GHz) and band 2 (0.9-1.8 GHz). These surveys are three-tiered aiming to observe a set of field of views (FoVs) on the sky at different depths: Wide Tier (WT), Deep Tier (DT), and Ultra-Deep Tier (UDT). In band 2, the sky levels (rms sensitivities) will be 1, 0.2, $0.05\mu\text{Jy}$ with FoVs of 1000, 10, 1 deg^2 in WT, DT, and UDT, respectively (Prandoni & Seymour 2015).

3. Thermal and non-thermal processes back to cosmic noon

The free-free and synchrotron components of the RC surface brightness of the main-sequence galaxies such as M51, NGC6946, and M33 are simulated back to cosmic noon ($z \sim 3$) taking into account the SKA1-MID band 2 angular resolution of 0.6 arcsec (corresponding to maximum sensitivity at 1.4 GHz in phase 1) and adding the sky levels of WT, DT, and UDT surveys as background noise (Ghasemi-Nodehi *et al.* 2022). These simulations make use of the available free-free emission maps of M51, NGC6946, and M33 obtained using de-reddened $\text{H}\alpha$ emission maps (Tabatabaei *et al.* 2013, 2022) tracing the thermal processes in the ionized ISM as well as their pure synchrotron maps tracing the non-thermal processes. Both processes can be detected in M51 and NGC6946 analogs back to cosmic noon, but they are hardly detected in low mass M33 analogs at $z > 0.5$ by the proposed SKA1 surveys. Hence, studies of dwarf galaxies at earlier cosmic times should wait for the phase 2 surveys. The ISM structures detected can include various galactic components such as spiral arms, clumps, and disks at $z < 1$ depending on if galaxies do not evolve in size (case 1, Fig 2) or whether they shrink with increasing redshift (case 2). Less structural details are detected in case 2 than case 1 at each specific redshift at $z > 0.15$. On the other hand, galaxies are brighter and thus more likely to be detected globally at higher redshifts in case 2. At $z > 1$, studies will be mainly limited to inner versus outer disk properties in both cases 1 and 2 at the resolution of this study.

4. Evolution of RC spectrum

The RC emission changes with frequency following a power-law relation, $\sim \nu^{-\alpha}$, with α the spectral index ($\alpha > 0$ in optically-thin regime) which is set by cosmic ray electron energy index if the contribution of the free-free emission is subtracted. As the synchrotron spectrum of a cosmic ray electron population is flatter at higher energies, it is expected that α changes locally depending on the location and environment (e.g., in star-forming

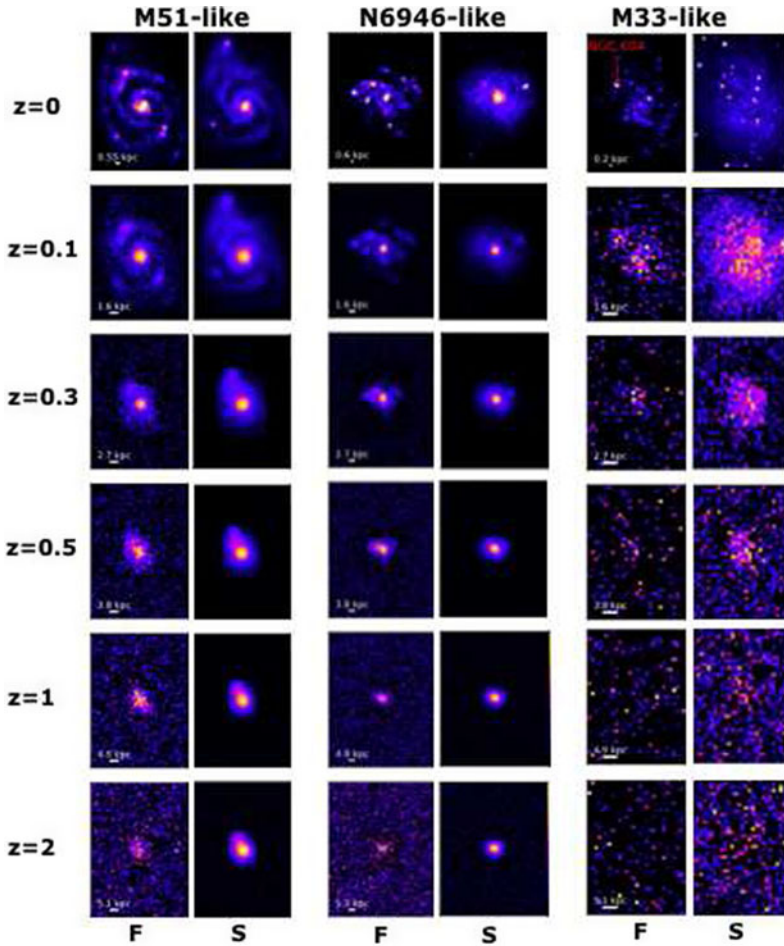


Figure 2. Simulated surface brightness maps of the free-free (F) and synchrotron emission (S) for M51, NGC 6946, and M 33 analogs as observed with the SKA1-MID UDT at the observed frequency of 1.4 GHz at selected redshifts z for case (1). First row ($z=0$) shows the actual thermal and non-thermal maps separated by combining the RC and de-reddened $H\alpha$ emissions (Ghasemi-Nodehi *et al.* 2022).

regions or diffuse ISM) and also globally from one galaxy to another depending on properties such as general star formation activities. Observations show that α is flatter in star-forming regions where these particles are injected and accelerated (Tabatabaei *et al.* 2013). Also, global studies show a flatter spectrum with increasing SFR surface density of normal star-forming galaxies (Tabatabaei *et al.* 2017). It is hence expected that cosmic rays become more powerful at the peak of SFR history at cosmic noon. Our predictions indeed show a flattening of the synchrotron spectrum with increasing z (Fig. 2). Hence, the role of cosmic ray electrons in the onset of winds and outflows deduced in galaxies like M33 (Tabatabaei *et al.* 2022) could have been even more significant in early galaxies.

5. Summary

The non-thermal synchrotron component of the RC emission traces cosmic ray electrons and magnetic fields- the energetic components of the ISM/IGM. Thus, mapping the synchrotron emission in galaxies over cosmic time is vital in galaxy evolution studies.

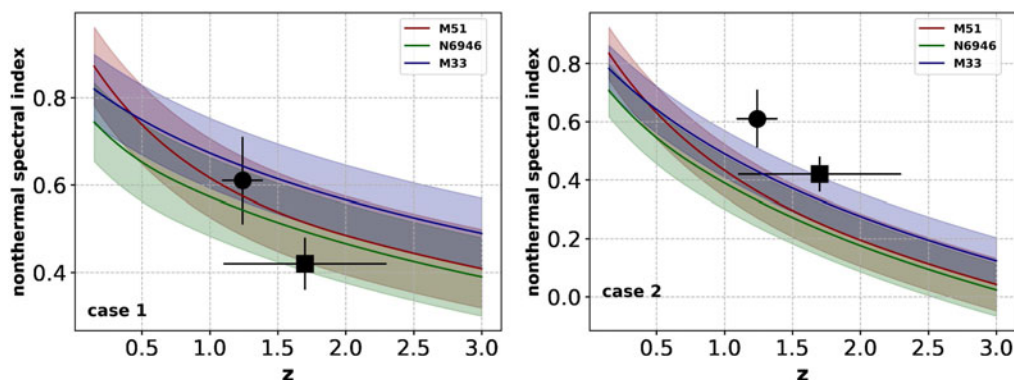


Figure 3. Evolution of the spectral index α_{nt} with redshift assuming no size evolution in the radio frequencies (case 1, *left*) and an evolution similar to that in the optical frequencies (case 2, *right*). Shaded bands show errors in the spectral indices. Points indicate the measurements based on observations (circle: [Murphy et al. 2017](#) and square: [Tisanić et al. 2019](#)) showing a better agreement with case 1.

This is uniquely possible through coordinated observations in the radio with SKA and the optical/near-infrared with JWST enabling us to study the role of the thermal and non-thermal processes in the formation and evolution of galactic structures, at least, back to cosmic noon as predicted by [Ghasemi-Nodehi et al. \(2022\)](#).

References

- Beck, R., 2007, *A&A*, 470, 539
- Colombo, D., Sanchez, S. F., Bolatto, A. D., et al. 2020, *A&A*, 644, 97
- Condon, J. J., Huang, Z. P., Yin, Q., F., & Thuan, T. X., 1991, *ApJ*, 378, 65
- Faber, S. M., Willmer, C. N. A., Wolf, C., et al. 2007, *ApJ*, 665, 265
- Ghasemi-Nodehi, M., Tabatabaei, F. S., Sargent, et al. 2022, *MNRAS*, 515, 1158
- Hassani, H., Tabatabaei, F., Hughes, A., et al. 2022, *MNRAS*, 510, 11
- Jakobsen, P., Ferruit, P., Alves de Oliveira, C., et al. 2022, *A&A*, 661, 80
- Murphy, E. J., Momjian, E., Condon, J. J., et al. 2017, *ApJ*, 839, 35
- Owen, E. R., Wu, K., Jin, X. et al. 2019, *A&A*, 626, 85
- Peng, Y., Maiolino, R., Cochrane, R., et al. 2015, *Nature*, 521, 192
- Pillai, T., Kauffmann, J., Tan, J. C., et al. 2015, *ApJ*, 799, 74
- Prandoni, I. & Seymour, N., 2015, 'Advancing Astrophysics with the SKA' (AASKA14) - Continuum Science Chapters, p67, arXiv:1412.6942
- Schaye, J., Crain, R. A., Bower, R. G., et al. 2015, *MNRAS*, 446, 52
- Schinnerer, E., Hughes, A., Leroy, A., et al. 2019, *ApJ*, 887, 49
- Schreiber, C., Pannella, M., Elbaz, D. et al. 2015, *A&A*, 575, 74
- Tabatabaei, F. S., Cotton, W., Schinnerer, E. et al. 2022, *MNRAS*, 517, 2990
- Tabatabaei, F. S., Minguez, P., Prieto, M. A., et al. 2018, *NatAs*, 2, 83
- Tabatabaei, F. S., Schinnerer, E., Krause, M. et al. 2017, *ApJ*, 836, 185
- Tabatabaei, F. S., Schinnerer, E., Murphy, E. J. et al. 2013, *A&A*, 552, 19
- Tisanić K., Smolčić V., Delhaize, et al. 2019, *A&A*, 621, 139
- Tacconi, L. J., Genzel, R., Saintonge, A., et al. 2018, *ApJ*, 853, 179
- van der Wel, A., Franx, M., van Dokkum, P. G., et al. 2014, *ApJ*, 788, 28